Inorg. Chem. **2005**, *44*, 5600–5611

Preparations and Characterizations of Bichromophoric Systems Composed of a Ruthenium Polypyridine Complex Connected to a Difluoroborazaindacene or a Zinc Phthalocyanine Chromophore

Fabrice Odobel* and Hervé Zabri

Laboratoire de Synthèse Organique, UMR CNRS 6513 and FR CNRS 2465, Faculté des Sciences et des Techniques de Nantes, BP 92208, 2 rue de la Houssinière, 44322 Nantes Cedex 03, France

Received January 18, 2005

This paper describes the synthesis of a new series of molecules composed of a ruthenium cation liganded by a chloro or a thiocyanato, a 4,4′-(diethoxycarbonyl)-2,2′-bipyridine, and a 2,2′:6′,2″-terpyridine substituted in its 4′ position by a difluoroborazaindacene or a zinc phthalocyanine. A set of conditions are reported to conveniently synthesize these dyads by a Stille cross-coupling reaction between the trimethyltin derivative of the organic chromophore and the corresponding ruthenium complex with 4′-bromo-2,2′:6′,2″-terpyridine and 4,4′-(diethoxycarbonyl)-2,2′-bipyridine. The dyads were studied by UV–visible absorption spectroscopy, steady-state fluorescence, and electrochemistry. The results of these studies indicate strong electronic coupling between the zinc phthalocyanine unit and the ruthenium complex but weakly electronically coupled systems in the case of dyads containing a difluoroborazaindacene unit. The new bichromophoric systems display strong absorbance in the visible spectrum. An efficient quenching of the fluorescence of the organic chromophore by the nearby ruthenium complex was also observed in all of the dyads. In dyads connected to the borazaindacene, excitation spectra indicate efficient photoinduced energy transfer from the borazaindacene to the ruthenium complex.

Introduction

There is currently an intense research effort to develop efficient molecular systems for solar energy conversion and storage.[1−6] Among the various approaches to photovoltaic implementation, dye-sensitized solar cells (DSSCs) represent a promising one because they are based on a simple technology. DSSCs are composed of a wide-band-gap semiconductor, generally titanium dioxide, that is covered by a dye whose major role is to absorb visible light.[7−9] Larger spectral overlapping between the absorption spectrum of the sensitizer and the solar spectrum on the Earth's surface is desirable to enhance the overall performance of the photovoltaic device. Ruthenium diimine complexes are among the most studied and the most efficient sensitizers tested so far.[9,10] Despite their efficiencies, the ruthenium polypyridine complexes display relatively low molar absorptivity and particularly weak absorbance in the red part of the solar spectrum (because of an usually large Stokes shift).[11] In contrast, organic dyes are often characterized by very intense molar absorption coefficients with absorption bands that can be found in any window of the whole solar spectrum. Although there exist recently some exceptions,[12−16] organic dyes are

* To whom correspondence should be addressed. E-mail: Fabrice.Odobel@chimie.univ-nantes.fr.

(1) Wasielewski, M. R. *Chem. Rev.* **1992**, *92*, 435−461.
(2) Gust, D.; Moore, T. A.; Moore, A. L. *Acc. Chem. Res.* **2001**, *34*, 40−48.
(3) Kurreck, H.; Huber, M. *Angew. Chem., Int. Ed. Engl.* **1995**, *34*, 849−866.
(4) Balzani, V. *Electron Transfer in Chemistry*; Wiley-VCH: Weinheim, Germany, 2001.
(5) Dürr, H.; Bossmann, S. *Acc. Chem. Res.* **2001**, *34*, 905−917.
(6) Bard, A. J.; Fox, M. A. *Acc. Chem. Res.* **1995**, *28*, 141−145.
(7) Hagfeldt, A.; Grätzel, M. *Acc. Chem. Res.* **2000**, *33*, 269−277.
(8) Grätzel, M. *Nature* **2001**, *414*, 338−344.
(9) Kalyanasundaram, K.; Grätzel, M. *Coord. Chem. Rev.* **1998**, *177*, 347−414.
(10) O'Regan, B.; Grätzel, M. *Nature* **1991**, *353*, 737−740.
(11) Kalyanasundaram, K. *Photochemistry of polypyridine and porphyrin complexes*; Academic Press: London, 1992.
(12) Hara, K.; Kurashige, M.; Ito, S.; Shinpo, A.; Suga, S.; Sayama, K.; Arakawa, H. *Chem. Commun.* **2003**, 252−253.
(13) Hara, K.; Sato, T.; Katoh, R.; Furube, A.; Ohga, Y.; Shinpo, A.; Suga, S.; Sayama, K.; Sugihara, H.; Arakawa, H. *J. Phys. Chem. B* **2003**, *107*, 597−606.
(14) Hara, K.; Tachibana, Y.; Ohga, Y.; Shinpo, A.; Suga, S.; Sayama, K.; Sugihara, H.; Arakawa, H. *Sol. Energy Mater. Sol. Cells* **2003**, *77*, 89−103.
(15) Hara, K.; Kurashige, M.; Dan-oh, Y.; Kasada, C.; Shinpo, A.; Suga, S.; Sayama, K.; Arakawa, H. *New J. Chem.* **2003**, *27*, 783−785.

10.1021/ic050078m CCC: $30.25
Published on Web 07/08/2005

usually poor sensitizers in DSSCs in comparison to transition-metal polypyridine complexes. For examples, porphyrins and phthalocyanines are high absorbing pigments in the visible spectrum, but several studies show that these dyes used in DSSCs offer a relatively modest overall photovoltaic performance.[17−24]

To capture light energy efficiently, nature has developed in the course of evolution a very efficient molecular system: the light-harvesting antenna.[25,26] Its role is to maximize the absorption cross section of the light source, in terms of both absorption coefficients and the window of the wavelengths that are collected. Photons of different colors are absorbed by the different pigments of the antenna, then the excitation energy is funneled to the special pair by very rapid and efficient energy transfers.[27] A variety of elegant structures have been prepared and significant light-harvesting efficiencies have been achieved with artificial antenna systems[28−40] since the pioneering works of Lehn[41] and Balzani.[42−44] However, there have been very few practical applications made with such molecular systems.

Scheme 1. Potential Principle of Operation of the Dyads Studied Here[a]

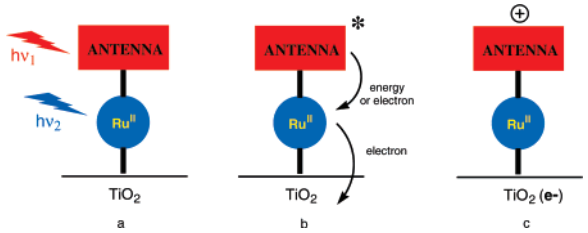

[a] Light excitation of the ruthenium complex with a photon of energy $h\nu_1$ results in electron injection in the conduction band of TiO_2. This step can be followed by a hole shift to the nearby antenna (leading to state c). Light excitation of the antenna with a photon of energy $h\nu_2$ can undergo energy or electron transfer to the ruthenium complex. In the case of electron transfer, the reduced ruthenium complex can also inject an electron into TiO_2. In the case of energy transfer, the sensitized ruthenium complex excited state can subsequently inject an electron into the conduction band of TiO_2.

The idea behind this work is to combine the high sensitizing efficiency of a ruthenium polypyridine complex[45,46] with the high absorbing property of an organic chromophore in order to generate a system with a large absorption cross section (Scheme 1).

Relevant examples include the trinuclear ruthenium complex prepared by Scandola and Bignozzi which showed a remarkable photovoltaic performance in DSSCs thanks to its high absorptivity.[47,48] More recently, Toma and co-workers reported porphyrin units that were coordinately bound to a ruthenium diimide complex to serve a similar purpose.[19,49] Despite these few examples, most compounds tested for semiconductor sensitization concern unimolecular systems, but a combination of distinct chromophores covalently linked are much less abundantly described in the literature.[50,51]

In this study, we report the synthesis and properties of a new series of dyads, in which a ruthenium polypyridine complex is connected to a high absorber, either a difluoroborazaindacene[52−54] (referred to as bodipy) or a zinc phthalocyanine[55−57] (referred to as ZnPc) (Figure 1). The ruthenium complex contains a bipyridinedicarboxylic acid ligand in its

(16) Hara, K.; Sayama, K.; Arakawa, H.; Ohga, Y.; Shinpo, A.; Suga, S. *Chem. Commun.* **2001**, 569−570.
(17) Nazeeruddin, M. K.; Humphry-Baker, R.; Officer, D. L.; Campbell, W. M.; Burrell, A. K.; Graetzel, M. *Langmuir* **2004**, *20*, 6514−6517.
(18) Fungo, F.; Otero, L. A.; Sereno, L.; Silber, J. J.; Durantini, E. N. *J. Mater. Chem.* **2000**, *10*, 645−650.
(19) Nogueira, A. F.; Furtado, L. F. O.; Formiga, A. L. B.; Nakamura, M.; Araki, K.; Toma, H. E. *Inorg. Chem.* **2004**, *43*, 396−398.
(20) Odobel, F.; Blart, E.; Lagrée, M.; Villieras, M.; Boujtita, H.; El Murr, N.; Carmori, S.; Bignozzi, C. A. *J. Mater. Chem.* **2003**, *13*, 502−510.
(21) Tachibana, Y.; Haque, S. A.; Mercer, I. P.; Durrant, J. R.; Klug, D. R. *J. Phys. Chem. B* **2000**, *104*, 1198−1205.
(22) He, J.; Benko, G.; Korodi, F.; Polivka, T.; Lomoth, R.; Akermark, B.; Sun, L.; Hagfeldt, A.; Sundstrom, V. *J. Am. Chem. Soc.* **2002**, *124*, 4922−4932.
(23) He, J.; Hagfeld, A.; Lindquist, S.-E. *Langmuir* **2001**, *17*, 2743−2747.
(24) Palomares, E.; Mart'nez-Dxc6, M. V.; Haque, S. A.; Torres, T. s.; Durrant, J. R. *Chem. Commun.* **2004**, 2112−2113.
(25) McDermott, G.; Prince, S. M.; Freer, A. A.; Hawthornthwaite-Lawless, A. M.; Papiz, M. Z.; Cogdell, R. J.; Isaacs, N. W. *Nature* **1995**, *374*, 517−521.
(26) Pullerits, T.; Sundström, V. *Acc. Chem. Res.* **1996**, *29*, 381−389.
(27) Sundström, V.; Pullerits, T.; Van Grondelle, R. *J. Phys. Chem. B* **1999**, *103*, 2327−2346.
(28) Choi, M.-S.; Aida, T.; Yamazaki, T.; Yamazaki, I. *Chem. Eur. J.* **2002**, *8*, 2668−2678.
(29) Choi, M.-S.; Yamazaki, T.; Yamazaki, I.; Aida, T. *Angew. Chem., Int. Ed.* **2004**, *43*, 150−158.
(30) Ambroise, A.; Kirmaier, C.; Wagner, R. W.; Loewe, R. S.; Bocian, D. F.; Holten, D.; Lindsey, J. S. *J. Org. Chem.* **2002**, *67*, 3811−3826.
(31) Li, F.; Yang, S. I.; Ciringh, Y.; Seth, J.; Martin, C. H.; Singh, D. L.; Kim, D.; Birge, R. R.; Bocian, D. F.; Holten, D.; Lindsey, J. S. *J. Am. Chem. Soc.* **1998**, *120*, 10001−10017.
(32) Holten, D.; Bocian David, F.; Lindsey Jonathan, S. *Acc. Chem. Res.* **2002**, *35*, 57−69.
(33) Loewe, R. S.; Tomizaki, K.-y.; Youngblood, W. J.; Bo, Z.; Lindsey, J. S. *J. Mater. Chem.* **2002**, *12*, 3438−3451.
(34) Adronov, A.; Frechet, J. M. J. *Chem. Commun.* **2000**, 1701−1710.
(35) Gilat, S. L.; Adronov, A.; Frechet, J. M. J. *Angew. Chem., Int. Ed.* **1999**, *38*, 1422−1427.
(36) Tyson, D. S.; Castellano, F. N. *Inorg. Chem.* **1999**, *38*, 4382−4383.
(37) Zhou, X.; Tyson, D. S.; Castellano, F. N. *Angew. Chem., Int. Ed.* **2000**, *39*, 4301−4305.
(38) Maus, M.; De, R.; Lor, M.; Weil, T.; Mitra, S.; Wiesler, U.-M.; Herrmann, A.; Hofkens, J.; Vosch, T.; Müllen, K.; De Schryver, F. C. *J. Am. Chem. Soc.* **2001**, *123*, 7668−7676.
(39) Weil, T.; Wiesler, U. M.; Herrmann, A.; Bauer, R.; Hofkens, J.; De Schryver, F. C.; Müllen, K. *J. Am. Chem. Soc.* **2001**, *123*, 8101−8108.
(40) Calzaferri, G.; Huber, S.; Huub, M.; Minkowski, C. *Angew. Chem., Int. Ed.* **2003**, *42*, 3732−3758.
(41) Jullien, L.; Canceill, J.; Valeur, B.; Bardez, E.; Lefevre, J.-P.; Lehn, J.-M.; Marchi-Artzner, V.; Pansu, R. *J. Am. Chem. Soc.* **1996**, *118*, 5432−5442.
(42) Prodi, L.; Maestri, M.; Ziessel, R.; Balzani, V. *Inorg. Chem.* **1991**, *30*, 3798−3802.
(43) Balzani, V.; Campagna, S.; Denti, G.; Juris, A.; Serroni, S.; Venturi, M. *Acc. Chem. Res.* **1998**, *31*, 26−34.
(44) Balzani, V.; Campagna, S.; Denti, G.; Juris, A.; Serroni, S.; Venturi, M. *Sol. Energy Mater. Sol. Cells* **1995**, *38*, 159−173.
(45) Bae, J. H.; Kim, D.; Kim, Y. I.; Kim, K.-J. *Bull. Korean Chem. Soc.* **1997**, *18*, 567−572.
(46) Maruthamuthu, P.; Anandan, S. *Sol. Energy Mater. Sol. Cells* **1999**, *59*, 199−209.
(47) Amadelli, R.; Argazzi, R.; Bignozzi, C. A.; Scandola, F. *J. Am. Chem. Soc.* **1990**, *112*, 7029.
(48) Bignozzi, C. A.; Argazzi, R.; Indelli, M. T.; Scandola, F. *Sol. Energy Mater. Sol. Cells* **1994**, *32*, 229−244.
(49) Nogueira, A. F.; Formiga, A. L. B.; Winnischofer, H.; Nakamura, M.; Engelmann, F. M.; Araki, K.; Toma, H. E. *Photochem. Photobiol. Sci.* **2004**, *3*, 56−62.
(50) Peter, K.; Wietasch, H.; Peng, B.; Thelakkat, M. *Polym. Prepr. (Am. Chem. Soc., Div. Polym. Chem.)* **2004**, *45*, 492−493.
(51) Peter, K.; Wietasch, H.; Peng, B.; Thelakkat, M. *Appl. Phys. A* **2004**, *79*, 65−71.
(52) Turfan, B.; Akkaya, E. U. *Org. Lett.* **2002**, *4*, 2857−2859.
(53) Ulrich, G.; Ziessel, R. *Tetrahedron Lett.* **2004**, *45*, 1949−1953.
(54) Goze, C.; Ulrich, G.; Charbonniere, L.; Cesario, M.; Prange, T.; Ziessel, R. *Chem. Eur. J.* **2003**, *9*, 3748−3755.

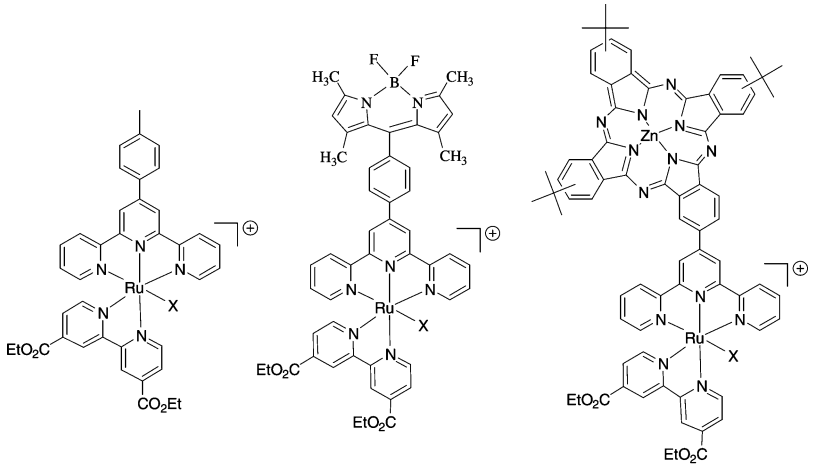

Figure 1. Structures of the molecules prepared in this study.

coordination sphere to subsequently allow for the immobilization of these dyads on a semiconductor electrode. It is indeed reported that similar ruthenium polypyridine complexes proved to be efficient sensitizers in DSSCs.[45,46,58] Besides the expected improved light-harvesting efficiency in a DSSC, dyads **3**−**6** could also lead to a potentially long-lived charge-separated state upon light excitation.[59−63] After electron injection into the conduction band of TiO_2, the ruthenium(III) complex could oxidize the nearby antenna by a charge shift process and lead to a new charge-separated state (state c in Scheme 1). The increasing distance between the electron in the conduction band of TiO_2 and the hole on the antenna will certainly be beneficial to slow the rate of the charge recombination reaction.

In the dyads described herein, the bodipy unit increases the molar absorption coefficient of the system in the metal-to-ligand charge-transfer (MLCT) region. Sensitizers with very high molar absorption coefficients could also be valuable for preparing a highly colored electrode with a very thin TiO_2 layer and could therefore be potentially useful for solid DSSCs.[64] The utilization of a low-surface-area TiO_2 film instead of a thick one could be beneficial to improve the wetting of the hole transport material in dry DSSCs.[65−68]

Herein, we describe the preparation of new bichromophoric ruthenium complexes connected to a bodipy or a ZnPc unit using an efficient synthetic strategy relying on a Stille cross-coupling reaction using polypyridineruthenium complexes as substrates. The absorption, emission, and excitation spectra along with the redox potentials of the new molecules were investigated and are reported in this paper.

Results and Discussion

Preparation of the Compounds. The preparation of dyads **3**−**6** required the synthesis of the new terpyridyl ligands **13** and **14** (Scheme 2). The key step for the preparation of the molecules presented here relies on a Stille cross-coupling reaction. This synthetic modular approach is very flexible and opens up the preparation of a large variety of dyads with different types of organic chromophores. From a retrosynthetic point of view, the disconnection for the preparation of the dyads **3**−**6** was made between the terpyridine unit and the antenna unit. At this stage, there remains the choice of the moiety that would bear the organotin group, either on the terpyridine unit or on the antenna (route A or route B in Scheme 2).

The two routes were tested because it was difficult to anticipate which one would give the highest yield. The synthesis of the 4′-stannylterpyridine **7** was earlier reported by Sauer.[69,70] However, we preferred to use the palladium-catalyzed stannylation of 4′-[[(trifluoromethyl)sulfonyl]oxy]-2,2′:6′,2″-terpyridine (**16**)[71] with hexamethylditin because of

(55) Kimura, M.; Hamakawa, T.; Muto, T.; Hanabusa, K.; Shirai, H.; Kobayashi, N. *Tetrahedron Lett.* **1998**, *39*, 8471−8474.
(56) Kimura, M.; Hamakawa, T.; Hanabusa, K.; Shirai, H.; Kobayashi, N. *Inorg. Chem.* **2001**, *40*, 4775−4779.
(57) Gonzalez-Cabello, A.; Vazquez, P.; Torres, T.; Guldi, D. M. *J. Org. Chem.* **2003**, *68*, 8635−8642.
(58) Zakeeruddin, S. M.; Nazeeruddin, M. K.; Pechy, P.; Rotzinger, F. P.; Humphry-Baker, R.; Kalyanasundaram, K.; Grätzel, M.; Shklover, V.; Haibach, T. *Inorg. Chem.* **1997**, *36*, 5937−5946.
(59) Argazzi, R.; Bignozzi, C. A.; Heimer, T. A.; Castellano, F. N.; Meyer, G. J. *J. Phys. Chem. B* **1997**, *101*, 2591−2597.
(60) Argazzi, R.; Bignozzi, C. A. *J. Am. Chem. Soc.* **1995**, *117*, 11815−11816.
(61) Bonhôte, P.; Moser, J.-E.; Humphry-Baker, R.; Vlachopoulos, N.; Zakeeruddin, S. M.; Walder, L.; Grätzel, M. *J. Am. Chem. Soc.* **1999**, *121*, 1324−1336.
(62) Christ, C. S.; Yu, J.; Zhao, X.; Palmore, T. R.; Wrighton, M. S. *Inorg. Chem.* **1992**, *31*, 4439−4440.
(63) Hirata, N.; Lagref, J.-J.; Palomares, E. J.; Durrant, J. R.; Nazeeruddin, M. K.; Gratzel, M.; Di Censo, D. *Chem. Eur. J.* **2004**, *10*, 595−602.
(64) Bach, U.; Lupo, D.; Comte, P.; Moser, J. E.; Weissortel, F.; Salbeck, J.; Spreitzer, H.; Grätzel, M. *Nature* **1998**, *395*, 583−585.
(65) Smestad, G. P.; Spiekermann, S.; Kowalik, J.; Grant, C. D.; Schwartzberg, A. M.; Zhang, J.; Tolbert, L. M.; Moons, E. *Sol. Energy Mater. Sol. Cells* **2003**, *76*, 85−105.
(66) Jäger, C.; Bilke, R.; Heim, M.; Haarer, D.; Karickal, H.; Thelakkat, M. *Synth. Met.* **2001**, *121*, 1543−1544.
(67) Bach, U.; Tachibana, Y.; Moser, J.-E.; Haque, S. A.; Durrant, J. R.; Grätzel, M.; Klug, D. R. *J. Am. Chem. Soc.* **1999**, *121*, 7445−7446.
(68) Gebeyehu, D.; Brabec, C. J.; Sariciftci, N. S.; Vangeneugden, D.; Kiebooms, R.; Vanderzande, D.; Kienberger, F.; Schindler, H. *Synth. Met.* **2001**, *125*, 279−287.
(69) Pabst, G. R.; Sauer, J. *Tetrahedron* **1999**, *55*, 5067−5088.
(70) Pabst, G. R.; Pfuller, O. C.; Sauer, J. *Tetrahedron* **1999**, *55*, 8045−8064.
(71) Potts, K. T.; Konwar, D. *J. Org. Chem.* **1991**, *56*, 4815−4816.

Scheme 2. Synthesis of the Terpyridinyl Ligands **13** and **14**

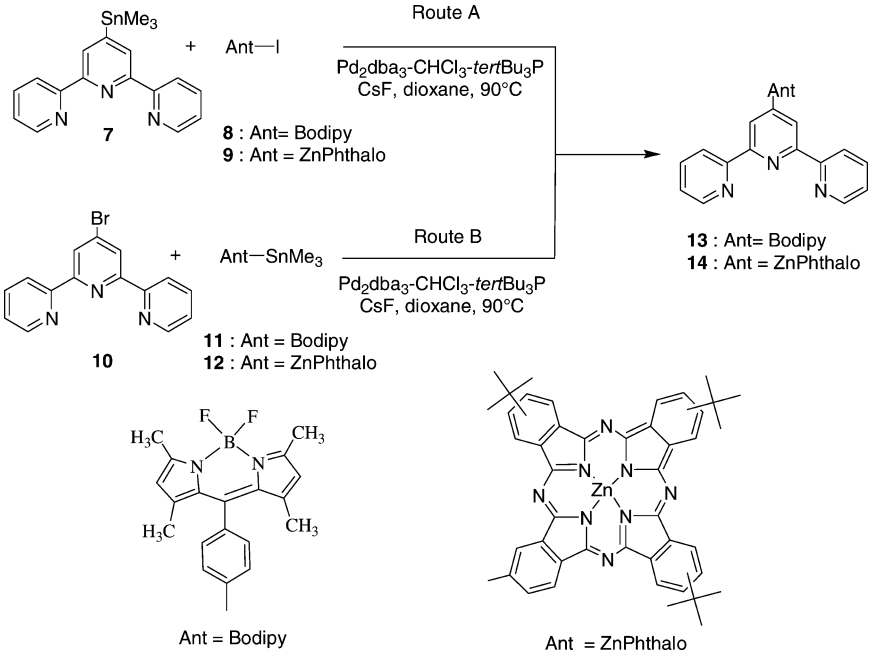

Scheme 3 [a]

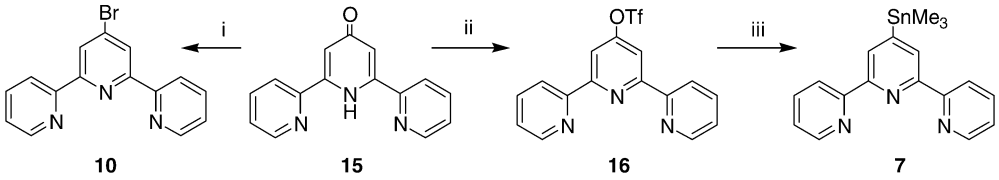

[a] Conditions and reagents: (i) $POBr_3$, PBr_5, 100 °C, 12 h (70%); (ii) $(TfO)_2O$, pyridine, 48 h, 90 °C (82%); (iii) Sn_2Me_6, dioxane, $Pd(PPh_3)_4$, LiCl (52%).

its easy access from the pyridone **15**,[71] which is also an intermediate for the preparation of the useful 4′-bromoterpyridine **10**[72] (Scheme 3).

Esterification of the pyridone **15** by triflic anhydride or bromination with the mixture phosphorus tribromide/phosphorus oxybromide according to literature procedures[71,72] led respectively to 4′-triflate terpyridine **16** and 4′-bromoterpyridine **10** with good yields. The 4′-triflate terpyridine **16** was transformed into 4′-stannylterpyridine **7** in a 58% yield using Hitchcock conditions.[73]

The same stannylation conditions applied to the known iodoborodiazaindacene **8**[74,75] or tri-*tert*-butyliodo-ZnPc **9**[76] afforded respectively the new stannanes **11** and **12** with yields over 90% in both cases (Scheme 4).

The Stille cross-coupling reaction for the synthesis of the ligand **13** was first performed with stannylterpyridine **7** and iodo-bodipy **8** using the conditions reported by Fu (dioxane, $Pd_2dba_3-CHCl_3$, $^tBu_3P$, CsF, 90 °C)[77] (route A, Scheme 2).

Scheme 4. Stannylation of the bodipy and ZnPc Antenna

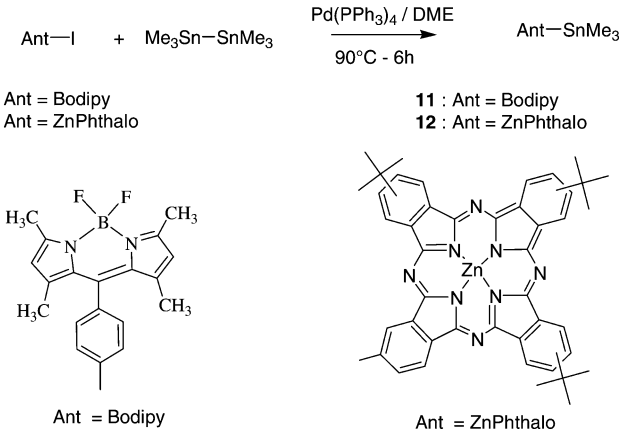

These reaction conditions led to the expected coupled product **13** with a 36% yield. This compound **13** was obtained with a higher yield when the reactive groups were inverted (route B, Scheme 2) because the same reaction conditions applied to 4′-bromoterpyridine **10** and stannyl-bodipy **11** afforded **13** with a 58% yield. The greater stability of the stannyl-bodipy over the stannylterpyridine **7** could be responsible for the higher yield of the latter reaction. Organometallics with pyridine derivatives are known to be less stable than those with electron-rich organic moieties.[78,79] It is noteworthy

(72) Uyeda, H. T.; Zhao, Y.; Wostyn, K.; Asselberghs, I.; Clays, K.; Persoons, A.; Therien, M. J. *J. Am. Chem. Soc.* **2002**, *124*, 13806−13813.
(73) Hitchcock, S. A.; Mayhugh, D. R.; Gregory, G. S. *Tetrahedron Lett.* **1995**, *36*, 9085−9088.
(74) Burghart, A.; Kim, H.; Welch, M. B.; Thoresen, L. H.; Reibenspies, J.; Burgess, K.; Bergstroem, F.; Johansson, L. B. A. *J. Org. Chem.* **1999**, *64*, 7813−7819.
(75) Thoresen, L. H.; Kim, H.; Welch, M. B.; Burghart, A.; Burgess, K. *Synlett* **1998**, 1276−1278.
(76) Maya, E. M.; Vazquez, P.; Torres, T. *Chem. Eur. J.* **1999**, *5*, 2004−2013.
(77) Littke, A. F.; Fu, G. C. *Angew. Chem., Int. Ed.* **1999**, *38*, 2411−2413.
(78) Mongin, F.; Queguiner, G. *Tetrahedron* **2001**, *57*, 5897.

Scheme 5 [a]

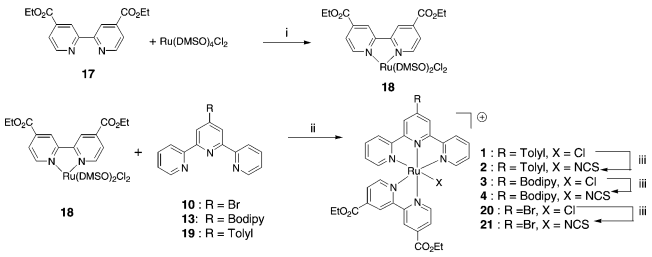

[a] Conditions: (i) $CHCl_3$, reflux, 10 h (70%); (ii) EtOH, H_2O, LiCl, 10 h, 90 °C (75%); (iii) KSCN, EtOH, H_2O (70%).

that the utilization of the classical conditions of Stille coupling[80,81] (toluene or DMF, $Pd(PPh_3)_4$, 90−120 °C) gave a lower yield for these transformations.

The preparation of the ligand **14** was more tedious. First, the coupling of 4′-stannylterpyridine **7** with iodotri-*tert*-butyl-ZnPc **9** failed (route A) using either classical conditions[81] (toluene, $Pd(PPh_3)_4$, 90−120 °C) or the Fu conditions.[77] The main products of this reaction were the terpyridine and the deiodinated phthalocyanine. The reverse coupling (route B, Scheme 2), namely, the reaction between the 4′-bromoterpyridine **10** and the stannylphthalocyanine **12**, enabled us to obtain the desired compound **14** but with a modest yield (18%). This disappointing result prompted us to explore another synthetic strategy to prepare these dyads. Anticipating that the terpyridine could deactivate the catalyst by coordination of the palladium, we decided to use preformed ruthenium complex **20** or **21** as a reagent instead of the 4′-bromoterpyridine **10** (Scheme 6). The preparation of the dyad **3** calls for mild metalation conditions for the preparation of the ruthenium complexes because the classical metalation conditions of polypyridine with ruthenium ($RuCl_3 \cdot nH_2O$ in refluxing DMF)[82,83] could be too harsh with some fragile ligands prepared in this study (especially ligands **13**). The overall synthetic approach for the preparation of the ruthenium complexes is summarized in Scheme 5.

First, the diethyl ester bipyridine **17**[84] was complexed with $Ru(DMSO)_4Cl_2$[85] by a gentle reflux in chloroform in a stoichiometric amount of these reagents. This reaction led to **18** as a mixture of two geometrical isomers *cis* and *trans*, which can be separated by column chromatography, but the mixture was used in the next step. The introduction of the terpyridine ligand on the ruthenium sphere can be satisfyingly performed by refluxing in ethanol the previous complex **18** with 1 equiv of the appropriate terpyridine. This strategy applied to the terpyridine ligands **10**, **13**, and **19** allowed one to generate the corresponding complexes **1**, **3**, and **20** in good yields after purification by column chromatography. It is noteworthy that, during the metalation step, we did not observe any decomposition of the bodipy unit or significant hydrolysis of the diethyl ester carboxylate groups. The chloro ligand in complexes **1**, **3**, and **20** can be substituted by thiocyanato by refluxing them with a slight excess of potassium thiocyanate in a mixture of ethanol/water.

Finally, the Stille cross-coupling reaction was successfully carried out with the ruthenium complexes **20** and **21** and the stannanes **11** and **12** (Scheme 6). Cross-coupling reactions directly involving an organometallic reagent with a complex containing a ligand substituted by a halide are far less developed than those using organic halides as substrates. Tor and co-workers[86,87] and more recently Ziessel and co-workers[88−90] reported the utilization of polypyridineruthenium complexes for a Sonogashira cross-coupling reaction with acetylenic derivatives. There are fewer examples in the literature describing Suzuki cross-coupling complexes bearing halide reagents,[88,91−93] and to the best of our knowledge, there is no report of a Stille reaction between tin derivatives and metallosynthons. We show here that the Stille cross-coupling reaction can be performed in satisfying yields using the metallosynthon complexes **20** and **21** directly. It is noteworthy that the catalytic system used here is particularly important to guarantee both a high rate and a good yield for this reaction. Other conditions were tested (DMF, $Pd(PPh_3)_4$, 110 °C, or dioxane, $Pd_2dba_3-CHCl_3$, $^tBu_3P$, CsF, 90 °C), but the completion of the reaction required a longer time ($t > 24$ h) and the yields were much lower (10−20%).

This synthetic strategy represents a potentially useful synthetic approach for the preparation of multicomponent systems containing a metallocomplex subunit because the coordination chemistry is performed separately in the early stage of the synthesis and it thus avoids running of the metalation step, which often requires harsh conditions not compatible with some fragile organic moieties.

UV−Visible Absorption Spectra. The spectroscopic characteristics of all new compounds are gathered in Table 1.

Spectra of the Ligands. For both ligands **13** and **14**, the spectrum is a linear combination of the spectra of the tolylterpyridine **19** and the antenna **8** or **9** (Figures 2 and 3 and Figures S1 and S2 in the Supporting Information). This indicates that there are few electronic interactions in the ground state of these compounds. In the spectrum of **13** or **14**, the $\pi-\pi^*$ transitions of the terpyridine unit are clearly

(79) Trecourt, F.; Breton, G.; Bonnet, V.; Mongin, F.; Marsais, F.; Queguiner, G. *Tetrahedron Lett.* **1999**, *40*, 4339−4342.
(80) Stille, J. K. *Angew. Chem., Int. Ed. Engl.* **1986**, *25*, 508−524.
(81) Stanforth, S. P. *Tetrahedron* **1998**, *54*, 263−303.
(82) Collin, J. P.; Gavina, P.; Heitz, V.; Sauvage, J. P. *Eur. J. Inorg. Chem.* **1998**, 1−14.
(83) Sauvage, J. P.; Collin, J. P.; Chambron, J. C.; Guillerez, S.; Coudret, C.; Balzani, V.; Barigelletti, F.; De Cola, L.; Flamigni, L. *Chem. Rev.* **1994**, *94*, 993−919.
(84) Hammarström, L.; Norrby, T.; Stenhagen, G.; Maartensson, J.; Aakermark, B.; Almgren, M. *J. Chem. Phys. B* **1997**, *101*, 7494−7504.
(85) Evans, I. P.; Spencer, A.; Wilkinson, G. *J. Chem. Soc., Dalton Trans.* **1973**, 204−209.
(86) Connors, P. J., Jr.; Tzalis, D.; Dunnick, A. L.; Tor, Y. *Inorg. Chem.* **1998**, *37*, 1121−1123.
(87) Tzalis, D.; Tor, Y. *J. Am. Chem. Soc.* **1997**, *119*, 852−853.
(88) Kozlov Denis, V.; Tyson Daniel, S.; Goze, C.; Ziessel, R.; Castellano Felix, N. *Inorg. Chem.* **2004**, *43*, 6083−6092.
(89) Ziessel, R.; Grosshenny, V.; Hissler, M.; Stroh, C. *Inorg. Chem.* **2004**, *43*, 4262−4271.
(90) Goze, C.; Kozlov, D. V.; Castellano, F. N.; Suffert, J.; Ziessel, R. *Tetrahedron Lett.* **2003**, *44*, 8713−8716.
(91) Aspley, C. J.; Williams, J. A. G. *New J. Chem.* **2001**, *25*, 1136−1147.
(92) Chodorowski-Kimmes, S.; Beley, M.; Collin, J.-P.; Sauvage, J.-P. *Tetrahedron Lett.* **1996**, *37*, 2963−2966.
(93) Bossart, O.; De Cola, L.; Welter, S.; Calzaferri, G. *Chem.−Eur. J.* **2004**, *10*, 5771−5775.

Scheme 6 . Preparation of Dyads **3**−**6** via the Stille Cross-Coupling Reaction

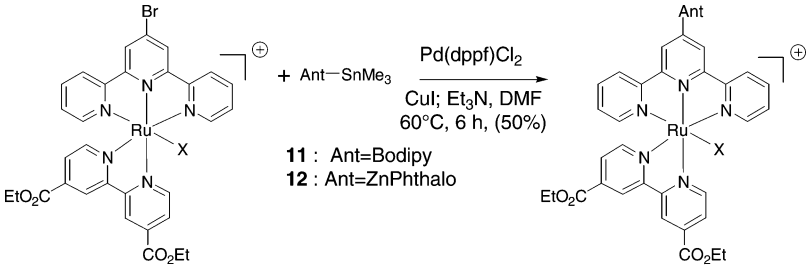

20 : R=Br, X= Cl
21 : R=Br, X= NCS

3 : Ant= Bodipy, X= Cl
4 : Ant= Bodipy, X= NCS
5 : Ant=ZnPhtlhalo, X= Cl
6 : Ant=ZnPhtlhalo, X= NCS

Table 1. Spectroscopic Absorption Characteristics of the Compounds Recorded in DMF

	absorption data [λ_{max}, nm (ϵ, M^{-1} cm^{-1})]
1	533 (15 600), 388 (9700) 316 (45 000)
2	522 (12 100), 384 (6900), 314 (36 600)
13	503 (26 400), 322 (7300), 277 (12 700)
3	504 (35 300), 371 (10 600), 315 (36 700)
4	505 (40 200), 380 (7400), 315 (33 600)
14	674 (76 600), 612 (22 500), 352 (29 000), 278 (41 000)
5	705 (87 000), 673 (73 300), 649 (36 000), 616 (22 000), 540 (14 000), 350 (57 600), 318 (60 000), 284 (40 000)
6	704 (91 000), 673 (78 000), 647 (34 400), 614 (23 000), 529 (13 900), 340 (58 000), 320 (63 000), 286 (44 200)

distinguished below 300 nm. The spectrum of **13** exhibits a supplementary absorption band in the visible (around 500 nm) that is attributed to a transition on the bodipy moiety. The ligand **14** displays intense absorption bands in the red area. The $\pi-\pi^*$ Soret transition toward the second singlet excited state of the zinc phthalocyanine appears at 352 nm and is slightly red shifted relative to the tetrakis-*tert*-butyl-ZnPc. The intense absorption bands in the visible region correspond to the Q bands of the zinc phthalocyanine, which are attributed to the $\pi-\pi^*$ transition to populate the first singlet excited state.[94]

Spectra of the Reference Ruthenium Complexes. The spectra of the reference complexes **1** and **2** are dominated by an intense $\pi-\pi^*$ transition of the polypyridyl ligand below 350 nm and by the well-known MLCT in the visible region (Table 1 and Figure S3 in the Supporting Information).[11] It is worth noting that the auxiliary chloro ligand induced a bathochromic shift (red) of the MLCT transition relative to that of the complexes **2** with the thiocyanato ligand. This effect is due to the destabilization of the d$-\pi$ Ru HOMO orbital by the electron-rich chloro ligand.

Spectra of the Dyads. The spectrum of the dyad **4** containing the bodipy antenna is illustrated in Figure 2 along with the spectra of the reference complex **2** and the ligand **13**.

The dyads **3** and **4** are simply the sum of the spectra of its components because of the weak interaction between bodipy and ruthenium polypyridine complexes. The most probable perpendicular orientation of the phenyl spacer with the bodipy unit interrupts the conjugation between the two motifs. The bodipy unit increases the light cross-sectional absorption in terms of intensification of the molar absorption because in the dyads **3** and **4** the molar absorptivity in the region of the MLCT transition is importantly enhanced compared to the reference ruthenium complex lacking the antenna (Figure 2 and Table 1).

The spectrum of the dyad **6** containing the zinc phthalocyanine is shown in Figure 3 along with the spectra of its molecular components.

In the dyads **5** and **6**, there exist ground state electronic interactions because we can notice a bathochromic shift of the maximum absorbance of the transitions relative to those of its constituents and also a splitting of the Q bands of the zinc phthalocyanine (Table 1 and Figure 3). The splitting of the Q bands is certainly a consequence of excitonic interactions between the dipole transitions of these latter transitions and that of the MLCT of the ruthenium complex. The excitonic coupling is only observed with the intense Q bands of the zinc phthalocyanine because its magnitude is proportional to the strength of the electronic transition.[95,96] This phenomenon is also very distance dependent, and therefore it is only observed when two chromophores are appended

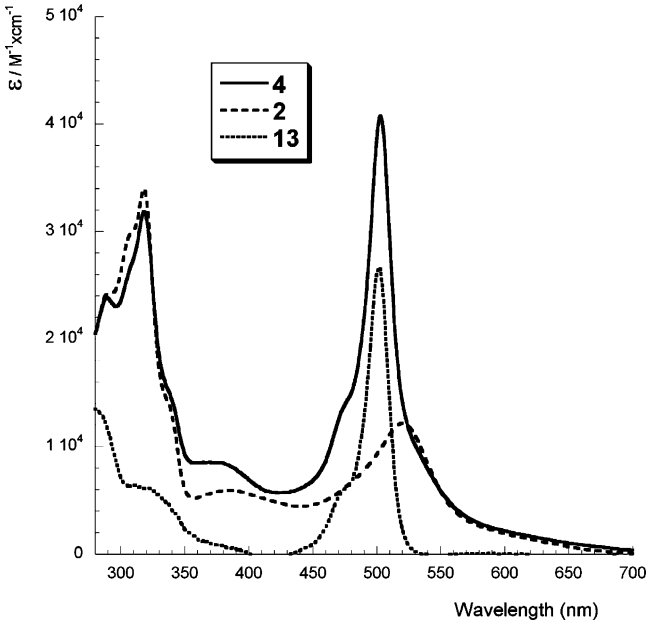

Figure 2. Overlay of the electronic absorption spectra recorded in DMF.

(94) Leznoff, C. C., Lever, A. B. P., Eds. *Phthalocyanines: Properties and Applications*; 1993.

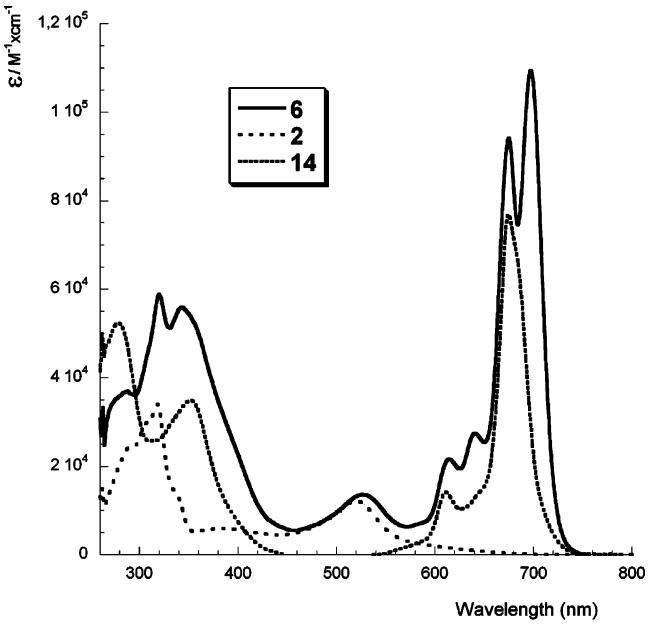

Figure 3. Overlay of the electronic absorption spectra recorded in DMF.

sufficiently close to one another so as the dipolar moments can interact through space by coulomb-type interactions.[95,96] Beautiful examples of excitonic coupling are given in the elegant meso−meso-linked porphyrin systems published by Osuka.[97−99] Similar Q-band splitting in zinc phthalocyanine and a ruthenium complex has been recently observed in a system prepared by Torres and co-workers.[57] It is noteworthy that no splitting was seen in the absorption spectrum of the ruthenium terpyridine−zinc phthalocyanine systems reported by Kimura and co-workers.[55,56] In this latter study, the methyl group in the 4′ position of the terpyridine probably forces the terpyridine unit to orient perpendicularly to the phthalocyanine macrocycle. Consequently, the dipolar moments of the two chromophores remain perpendicular and the interaction is null. Here in the dyads **5** and **6**, the molecules may adopt a more planar configuration, which allows for larger electronic interactions in the ground state. The presence of the zinc phthalocyanine unit on the ruthenium complex in the dyads **5** and **6** increases importantly the absorption cross section because the Q bands of the organic dye bring about an intense absorbance in the 600−720 nm window, where the ruthenium complex displays a very low extinction coefficient (Figure 3).

Electrochemical Study. The redox potentials of each electroactive unit in the dyads **3**−**6** were measured by cyclic voltammetry and confirmed by differential pulse voltammetry. The half-wave redox potentials ($E_{1/2}$) are summarized in Table 2.

Table 2. Electrochemical Study Performed in a Dry Deaerated Dichloromethane Solution Containing Bu_4NPF_6 (0.15 mol L^{-1}) as the Supporting Electrolyte with a Scan Rate of 100 mV/s[a]

	$E_{1/2}$, V			
	$Ant^{\bullet+}$/Ant	Ru^{III}/Ru^{II}	Ant/$Ant^{\bullet-}$	bipy(0/1−)
1		0.96		−1.17
2		1.03 (irr)		−1.17
13	1.18		−1.28	
3	1.10	0.88	−1.20 (bi)	−1.20 (bi)
4	1.16	1.03 (irr)	−1.13 (bi)	−1.13 (bi)
14	0.62		−1.06	
5	0.70	1.01	−1.03	−1.23
6	0.69	1.07 (irr)	−1.02	−1.18

[a] $E_{1/2}$ represents the average of the cathodic and anodic peak potentials. Irr = irreversible. Working electrode: Pt wire. Bi = bielectronic process.

The attribution of the electrochemical process was made according to the potentials measured on the model compounds. Ligands **13** and **14** exhibit one oxidation wave and one reduction wave located at potentials that are in agreement with similar compounds.[56,74,94,100] The bodipy chromophore is a moderate electron donor, whereas the zinc phthalocyanine is a good electron donor that can be potentially oxidized by the ruthenium complex. The oxidation on the reference complexes **1** and **2** was attributed to the metal-centered reaction Ru^{III}/Ru^{II}, as was usually observed for this type of complex.[101] Generally, the complexes liganded by the chloro ligand were slightly easier to oxidize than the thiocyanato analogues because of the known higher σ- and π-electron-donor character of the chloro ligand. The complexes **2**, **4**, and **6** containing the thiocyanato auxiliary ligand display irreversible oxidation probably because of the oxidative decomposition of the thiocyanato ligand into cyano, as observed with other ruthenium complexes.[102,103] In complexes **1**−**4**, the first reduction process arises most certainly on the bipyridine because it is the ligand that bears the lowest LUMO orbitals because of the presence of the two electron-withdrawing carboxylate substituents.[104] This assumption is supported by the fact that in the dyads **3** and **4** the reduction of the ruthenium complexes and that of the antenna arose at similar potentials in a wide bielectronic wave (Table 2). If the reduction of the polypyridine ligand were centered on the terpyridine unit, an important cathodic shift would have been expected for the second reduction process as a result of the accumulation of two negative charges in proximity. As a result, the accurate half-potential value of each reduction process was difficult to determine because of the occurrence of the two reduction processes at similar potentials. In the dyads **5** and **6**, the close proximity and the electronic interactions between the ZnPc and the ruthenium complex

(95) Kasha, M. *Radiat. Res.* **1963**, *20*, 55−70.
(96) Kasha, M.; Rawls, H. R.; El-Bayoumi, M. A. *Pure Appl. Chem.* **1965**, *11*, 371−392.
(97) Piet, J. J.; Taylor, P. N.; Anderson, H. L.; Osuka, A.; Warman, J. M. *J. Am. Chem. Soc.* **2000**, *122*, 1749−1757.
(98) Kim, Y. H.; Jeong, D. H.; Kim, D.; Jeoung, S. C.; Cho, H. S.; Kim, S. K.; Aratani, N.; Osuka, A. *J. Am. Chem. Soc.* **2001**, *123*, 76−86.
(99) Yoshida, N.; Ishizuka, T.; Osuka, A.; Jeong, D. H.; Cho, H. S.; Kim, D.; Matsuzaki, Y.; Nogami, A.; Tanaka, K. *Chem. Eur. J.* **2003**, *9*, 58−75.
(100) Wan, C.-W.; Burghart, A.; Chen, J.; Bergstroem, F.; Johansson, L. B. A.; Wolford, M. F.; Kim, T. G.; Topp, M. R.; Hochstrasser, R. M.; Burgess, K. *Chem.−Eur. J.* **2003**, *9*, 4430−4441.
(101) Eskelinen, E.; Luukkanen, S.; Haukka, M.; Ahlgren, M.; Pakkanen, T. A. *J. Chem. Soc., Dalton Trans.* **2000**, 2745−2752.
(102) Wolfbauer, G.; Bond, A. M.; MacFarlane, D. R. *Inorg. Chem.* **1999**, *38*, 3836−3846.
(103) Cecchet, F.; Gioacchini, A. M.; Marcaccio, M.; Paolucci, F.; Roffia, S.; Alebbi, M.; Bignozzi, C. A. *J. Chem. Phys. B* **2002**, *106*, 3926−3932.
(104) Pichot, F.; Beck, J. H.; Elliott, C. M. *J. Phys. Chem. A* **1999**, *103*, 6263−6267.

Table 3. Spectroscopic Emission Characteristics of the Compounds and Free Enthalpy (ΔG_{Ent}) of the Singlet to Triplet Energy Transfer Process from the Antenna to the Ruthenium Complex

	λ_{em}(77 K),[a] nm	λ_{em}(RT),[b] nm	Φ_f[c]	E_{00}(^{1}Ant*),[d] eV	E_{00}(^{3}MLCT*),[e] eV	ΔG_{Ent}, eV
1	729	819			1.70	
2	694	794			1.78	
13	508	512	0.70	2.45		
3	730, 760	514, 819	0.003	2.45	1.70	−0.75
4	700, 760	514, 798	0.003	2.45	1.77	−0.68
14	686, 712, 758	692, 762	0.24	1.81		
5	694, 732, 775	702, 771	0.010	1.77	1.69	−0.08
6	689, 707, 781	708, 781	0.010	1.77	1.75	−0.02

[a] Recorded in EtOH/CH_2Cl_2 = 95/5. [b] Recorded in DMF. [c] Fluorescence quantum yield measured in DMF at room temperature (RT). [d] E_{00}(^{1}Ant*): singlet excited state of the antenna, calculated from the wavelength at the intersection of the room-temperature absorption and emission spectra. [e] E_{00}(^{3}MLCT*): triplet excited state of the ruthenium complex, calculated from the maximum emission of the first emission band of the complex recorded at 77 K. $\Delta G_{Ent} = E_{00}(^3\text{MLCT*}) - E_{00}(^1\text{Ant*})$.

induce an anodic shift of the oxidation redox potentials of the antenna (Table 2). This is consistent with the results of the UV−vis absorption spectroscopy, which indicates stronger interacting chromophores in the case of the dyads **5** and **6** containing the zinc phthalocyanine.

Steady-State Luminescence Spectroscopy. The steady-state luminescence spectra of the dyads and the reference compounds have been recorded at room temperature and in a frozen matrix in order to determine the energy of each excited state and to investigate the effects of the neighboring ruthenium complex on the excited state of the antenna. From these data, the free enthalpy of the photoinduced energy-transfer process was calculated (Table 3).

The fluorescence emission wavelength and the quantum yield of the uncomplexed antenna **13** and **14** are in agreement with the data reported for similar dyes,[54,105,106] indicating few perturbations of the antenna excited state by the terpyridinyl fragment. Upon metalation by ruthenium, the energy of the ZnPc ligand **14** is slightly decreased, whereas the energy of the bodipy unit is not modified. This is in line with the UV−vis absorption and electrochemical studies, which indicate that the dyads **5** and **6** are more strongly electronically coupled than the dyads **3** and **4**.

It is important to note that, in the ruthenium complexes of **1**−**6**, the presence of the auxiliary ligand chloro or thiocyanato and the two electron-withdrawing ester groups on the bipyridine decreases substantially the energy of the MLCT excited state (≈1.7−1.8 eV), which is lower than that of a regular ruthenium trisbipyridine (2.1 eV).[107] As a result, in the dyads **3** and **4**, there exists a clear significant gradient for energy transfer to form the triplet excited state of the ruthenium complex from the singlet excited state of the antenna (Table 3). In complexes **1**−**6**, the phosphorescence emission and consequently the 0−0 energy [E_{00}(^{3}MLCT*)] of the MLCT is almost independent of the substituents borne by the terpyridine ligand (Table 3). This

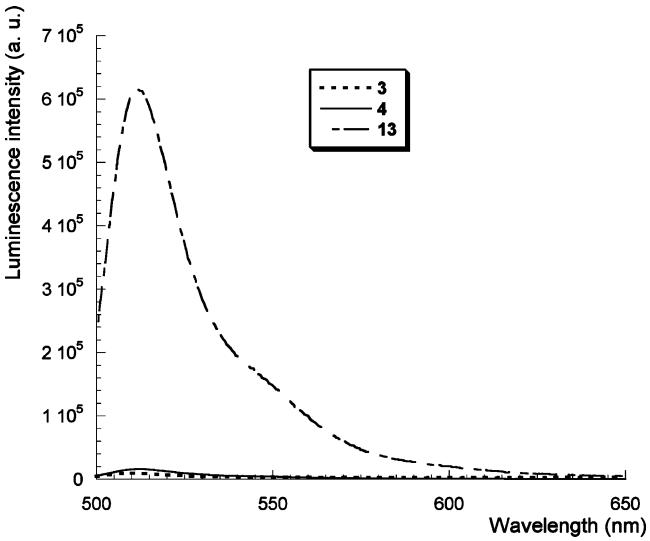

Figure 4. Overlay of the corrected emission spectra recorded in deaerated DMF with matched absorbance. Excitation wavelength: 490 nm.

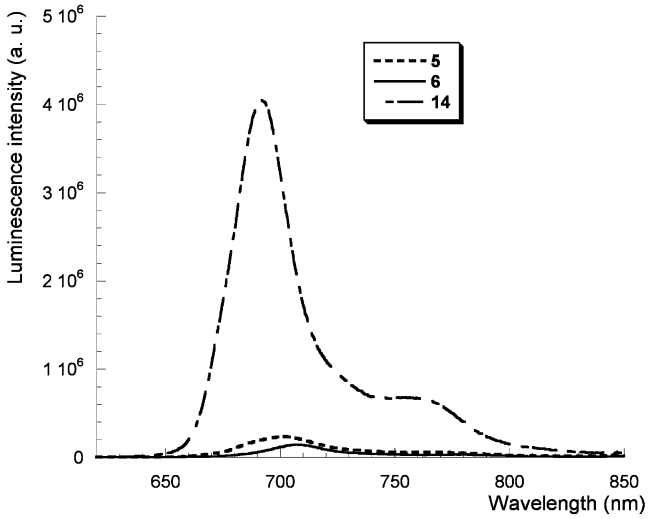

Figure 5. Overlay of the corrected emission spectra recorded in deaerated DMF with matched absorbance. Excitation wavelength: 614 nm.

result strongly implies that the LUMO orbital of the ruthenium complex is probably mostly localized on the 4,4′-(diethoxycarbonyl)-2,2′-bipyridine, which is thus the electron-acceptor ligand of the MLCT excited state. The corrected steady-state luminescence spectra of the dyads **3**−**6** along with those of the uncomplexed antennas **13** and **14** are shown in Figures 4 and 5.

The steady-state luminescence spectra (Figures 4 and 5) clearly show that the first singlet excited state of both antennas in all of the dyads **3**−**6** is strongly quenched by the appended ruthenium complex because the residual fluorescence of the antenna corresponds to less than 5% of the luminescence of the uncomplexed antennas **13** and **14**. In the dyads **3** and **4**, photoinduced energy transfer from the antenna singlet excited state to the triplet MLCT of the ruthenium complex is a thermodynamically allowed process.

A good estimation of the efficiency of the energy transfer can be inferred from the examination of the excitation spectra and the absorption spectra (Figure 6). The excitation spectra of the dyads **3** and **4** feature the shape of the absorption

(105) Leznoff, C. C., Lever, A. B. P., Eds. *Phthalocyanines: Properties and Applications*; 1989.
(106) Chen, J.; Burghart, A.; Derecskei-Kovacs, A.; Burgess, K. *J. Org. Chem.* **2000**, *65*, 2900−2906.
(107) Durham, B.; Caspar, J. V.; Nagle, J. K.; Meyer, T. J. *J. Am. Chem. Soc.* **1982**, *104*, 4803−4810.

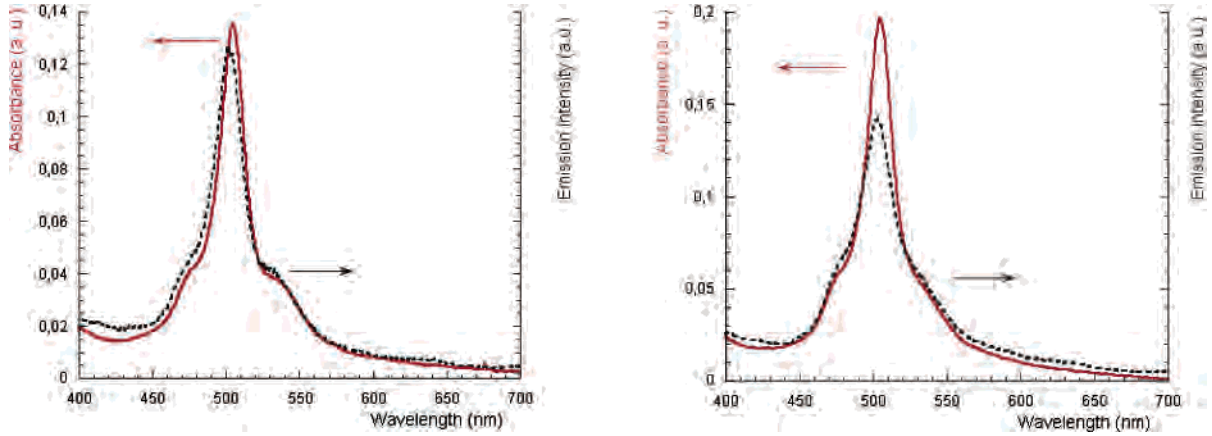

Figure 6. Normalized absorption (solid line) and corrected excitation spectra (dotted line) of dyad **3** (left, $\lambda_{em} = 800$ nm) and dyad **4** (right, $\lambda_{em} = 770$ nm) recorded at room temperature in a degassed DMF solution.

spectra, suggesting that photons absorbed by the borazaindacene moiety are indeed funneled to the appended ruthenium complex. On the basis of the intensity ratio of the excitation and absorption spectra on the maximum absorbance of the bodipy unit (504 nm), a 93% and 73% energy-transfer quantum yield can be respectively calculated for the dyads **3** and **4**.[108,109] The larger antenna effect observed in dyad **3** compared to dyad **4** most probably reflects the larger driving force in the former dyad (Table 3). The reduced energy-transfer quantum yield observed in dyad **4** can certainly be ascribed to photoinduced electron transfer and/or singlet to triplet intersystem crossing that may occur in parallel with energy transfer.

In the dyads **5** and **6**, the driving force for the photoinduced singlet to triplet energy transfer is weak compared to that in the dyads **3** and **4** (Table 3). Besides this, the poor spectral overlapping integral between the fluorescence spectrum of the phthalocyanine unit and the MLCT absorption band of the ruthenium complex renders energy transfer by the Förster mechanism[110,111] unlikely. The proximity of the two units and the strong electronic coupling observed in the dyads **5** and **6** does not, however, forbid energy transfer following the Dexter mechanism.[112] Furthermore, very efficient singlet to triplet energy transfer between an organic chromophore and the ruthenium bisterpyridine complex, exhibiting a very weak spectroscopic overlap integral, has been previously reported in some molecular dyads.[113−115] However, the strong overlap between the phthalocyanine fluorescence and the broad phosphorescence of the ruthenium complex prevents the utilization of the excitation spectra of the dyads **5** and **6** to assess the efficiency of the energy transfer (Figure S4 in the Supporting Information). In these dyads, if energy transfer does not occur, electron transfer or intersystem crossing are the only alternative quenching processes. If intersystem crossing is the main deactivation process, it is clear that the dyads will have poor efficiency in DSSCs. On the other hand, if electron transfer occurs, the ruthenium complex will be reduced, and it could certainly inject electrons to TiO_2 because the driving force for this process is even higher than that from the MLCT excited state (Scheme 1). It is worth noting that efficient photoinduced electron transfer has recently been reported by Holten and co-workers in a system consisting of a zinc porphyrin linked in a ruthenium trisbipyridine complex.[116] However, the univocal understanding of the deactivation pathway of the antenna excited state requires a detailed photophysical study with time-resolved luminescence and especially with transient absorption spectroscopy, but this is beyond the scope of this work.

Conclusions

In this work, we have synthesized and characterized new ligands and new ruthenium polypyridine complexes connected to a ZnPc or a bodipy chromophore. We have shown that a Stille cross-coupling reaction can be conducted directly with a metallosynthon such as **20** or **21** and an organotin reagent in mild conditions. This paper outlines a valuable strategy for the synthesis of ruthenium polypyridine−organic dyads containing a fragile organic moiety.

The electronic absorption spectra of the dyads revealed that the dyads containing the bodipy antenna are weakly coupled and exhibit intensification of the molar absorption coefficient within the MLCT region (around 500 nm). Strong electronic coupling can be observed in the spectra of the dyads **5** and **6** containing the ZnPc chromophore and was confirmed by the electrochemical and luminescence studies. Furthermore, these dyads absorb light in the large part of the visible spectrum from 300 to 720 nm with particularly a

(108) Stryer, L.; Haugland, R. P. *Proc. Natl. Acad. Sci. U.S.A.* **1967**, *58*, 719−726.
(109) Shortreed, M. R.; Swallen, S. F.; Shi, Z.-Y.; Tan, W.; Xu, Z.; Devadoss, C.; Moore, J. S.; Kopelman, R. *J. Phys. Chem. B* **1997**, *101*, 6318−6322.
(110) Förster, T. *Ann. Phys.* **1948**, *2*, 55−75.
(111) Förster, T. *Energy Commun.* **1965**, FSU-2690-18, 61.
(112) Dexter, D. L. *J. Phys. Chem.* **1953**, *21*, 836−852.
(113) Flamigni, L.; Barigelletti, F.; Armaroli, N.; Ventura, B.; Collin, J.-P.; Sauvage, J.-P.; Williams, J. A. G. *Inorg. Chem.* **1999**, *38*, 661−667.
(114) Flamigni, L.; Armaroli, N.; Barigelletti, F.; Balzani, V.; Collin, J.-P.; Dalbavie, J.-O.; Heitz, V.; Sauvage, J.-P. *J. Phys. Chem. B* **1997**, *101*, 5936−5943.
(115) Benniston, A. C.; Chapman, G. M.; Harriman, A.; Mehrabi, M. *J. Phys. Chem. A* **2004**, *108*, 9026−9036.
(116) Ambroise, A.; Wagner, R. W.; Rao, P. D.; Riggs, J. A.; Hascoat, P.; Diers, J. R.; Seth, J.; Lammi, R. K.; Bocian, D. F.; Holten, D.; Lindsey, J. S. *Chem. Mater.* **2001**, *13*, 1023−1034.

high molar absorption coefficient in the red part [for comparison, ϵ(black dye)[117,118] $\approx$ 4200 dm^3 mol^{-1} cm^{-1} at 700 nm, whereas ϵ(**6**) = 105 000 dm^3 mol^{-1} cm^{-1} at 700 nm]. The steady-state luminescence study indicates that in all of the dyads the singlet excited state of the organic antenna is strongly quenched by the presence of the ruthenium center. In the dyads **3** and **4**, containing the bodipy unit, the excitation spectra demonstrate that energy transfer is the major deactivation process of the antenna excited state. However, the univocal understanding of the photophysical behavior of the dyads **3**−**6** requires a detailed photophysical study that will be addressed in a future work.

Experimental Section

General Methods. ^{1}H NMR spectra were recorded on a Bruker, an Avance 300 MHz, or an ARX 400 MHz spectrometer. Chemical shifts for ^{1}H NMR spectra are referenced relative to residual protium in the deuterated solvent ($CDCl_3$ = 7.26 ppm; DMSO-d_6 = 2.49 ppm). Mass spectra were recorded on a EI-MS HP 5989A spectrometer or on a JMS-700 (JEOL LTD, Akishima, Tokyo, Japan) double-focusing mass spectrometer of reversed geometry equipped with an electrospray ionization source. Fast atom bombardement mass spectroscopy (FAB-MS) analyses were performed in a *m*-nitrobenzyl alcohol matrix on a ZAB−HF−FAB spectrometer. MALDI-TOF analyses were performed on an Applied Biosystems Voyager DE-STR spectrometer in positive linear mode at 20-kV acceleration voltage with α-cyano-4-hydroxycinnamic acid as the matrix. UV−visible absorption spectra were recorded on a UV-2401PC Shimadzu spectrophotometer. Fluorescence spectra were recorded on a SPEX Fluoromax fluorimeter and were corrected for the wavelength-dependent response of the detector system. The fluorescence quantum yield was calculated using 4,4-difluoro-8-(4′-iodophenyl)-1,3,5,7-tetramethyl-4-bora-3a,4a-diaza-*s*-indacene as a reference (Φ_f = 0.64 in $CHCl_3$)[106] and the following equation:

$$\Phi = \Phi_{ref}\{F(\lambda)[1 - \exp(-A_{ref}\ln 10)]n^2\}/\{F_{ref}(\lambda)[1 - \exp(-A\ln 10)]n_{ref}{}^2\}$$

where A, n, and $F(\lambda)$ denote the absorbance at the excitation wavelength, the refractive index of the solvent, and the area below the emission band of the corrected emission spectrum.

The electrochemical measurements were performed with a potentiostat−galvanostat MacLab model ML160 controlled by resident software (Echem v1.5.2 for Windows) using a conventional single-compartment three-electrode cell. The working electrode was a Pt wire of 10 mm long, the auxiliary was a Pt wire, and the reference electrode was the saturated potassium chloride calomel electrode (SCE). The supported electrolyte was 0.15 M Bu_4NPF_6 in dichloromethane, and the solutions were purged with argon before the measurements. All potentials are quoted relative to SCE. In all of the experiments, the scan rate was 100 mV/s for cyclic voltammetry and 15 Hz for pulse voltammetry.

Thin-layer chromatography (TLC) was performed on aluminum sheets precoated with Merck 5735 Kieselgel 60F_{254}. Column chromatography was carried out either with Merck 5735 Kieselgel 60F (0.040−0.063 mm mesh) or with SDS neutral alumina (0.05−0.2 mm mesh). Air-sensitive reactions were carried out under argon in dry solvents and glassware. Chemicals were purchased from Aldrich and used as received. Compounds tetrakis(triphenylphosphine)palladium,[119] 4′-bromo-2,2′:6′,2″-terpyridine (**10**),[72] 4′-[[(trifluoromethyl)sulfonyl]oxy]-2,2′:6′,2″-terpyridine (**16**),[71] 4,4-difluoro-8-(4′-iodophenyl)-1,3,5,7-tetramethyl-4-bora-3a,4a-diaza-*s*-indacene (**11**),[74,75] tri-*tert*-butyliodophthalocyaninatozinc(II) (**9**),[76] and 4,4′-(diethoxycarbonyl)-2,2′-bipyridine (**17**)[84] were prepared according to literature methods.

4′-(Trimethylstannyl)-2,2′:6′,2″-terpyridine (7). A sealed tube was charged with **16** (1.16 g, 3 mmol) and lithium chloride (0.39 g, 9 mmol) in 30 mL of dry dioxane. The mixture was degassed by pumping and flushing with argon on the vacuum line. Tetrakis(triphenylphosphine)palladium (0.35 g, 0.3 mmol) and hexamethylditin (1 g, 3 mmol) were added, and the mixture was heated to 110 °C for 16 h. After cooling to room temperature, the solution was filtered and the solid was washed with dichloromethane. The filtrate was purified by column chromatography on neutral alumina gel with petroleum ether/dichloromethane (100/0 to 90/10) as the eluent to give a white solid (0.63 g, 52%).

^{1}H NMR ($CDCl_3$, 300 MHz): δ 0.42 (s, 9H, J_{Sn-H} = 28 Hz), 7.32 (ddd, 2H, J = 5.7, 7.2, and 0.9 Hz), 7.86 (ddd, J = 7.9, 7.2, and 1.1 Hz, 2H), 8.58 (s, 2H), 8.61 (d, J = 7.9 Hz, 2H), 8.72 (m, 2H). MS (EI): *m*/*z* (%) 397 (28) ($M^{\bullet+}$), 382 (100).

4,4-Difluoro-8-[4′-(trimethylstannyl)phenyl]-1,3,5,7-tetramethyl-4-bora-3a,4a-diaza-*s*-indacene (11). A mixture of **8** (0.5 g, 1.11 mmol), hexamethylditin (540 mg, 1.6 mmol), and tetrakis(triphenylphosphine)palladium(0) (160 mg, 0.11 mmol) in 25 mL of dimethoxyethane was heated at 90 °C under an argon atmosphere for 15 h. The resulting brown mixture was evaporated in a vacuum until dryness. The resulting solid was purified by column chromatography over silica gel (eluent: petrol ether/dichloromethane/triethylamine = 80/16/4), affording a bright orange solid (480 mg, 90%).

^{1}H NMR ($CDCl_3$, 300 MHz): δ 7.57 (d, J = 7.8 Hz, J_{Sn-H} = 6.8 Hz, J_{Sn-H} = 49.6 Hz, 2H), 7.22 (d, J = 7.8 Hz, 2H), 5.97 (s, 2H), 2.55 (s, 6H), 1.38 (s, 6H), 0.34 (s, J_{Sn-H} = 55.2 Hz, 9H). MS (EI): *m*/*z* (%) 488.50 (100, M + H^+), 473.45 (38), 458.45 (63), 443.40 (28), 304.40 (63), 288.35 (63).

Trimethylstannyl Tri-*tert*-butyliodophthalocyaninatozinc(II) (12). A sealed tube was charged with tri-*tert*-butyliodo-ZnPc (**9**; 120 mg, 0.14 mmol), hexamethylditin (70 mg, 0.21 mmol), and tetrakis(triphenylphosphine)palladium(0) (30 mg, 0.025 mmol) in 10 mL of dimethoxyethane. The mixture was degassed with argon three times and was heated to 100 °C under an argon atmosphere for 6 h. The crude reaction was evaporated to dryness, and the residue was recrystallized from hot ethanol, cooled to room temperature, and filtered, affording a deep blue powder (105 mg, 80%).

^{1}H NMR ($CDCl_3$, 300 MHz): δ 7.96 (m, 8H), 7.69 (m, 4H), 1.77 (s, 27H), 0.66 (s, J_{Sn-H} = 55 Hz, 9H). HRMS (ES-MS): calcd for $C_{47}H_{48}N_8SnZn$ ($M^{\bullet+}$ + H^+), 909.2394; found, 909.2388.

(117) Nazeeruddin, M. K.; Pechy, P.; Graetzel, M. *Chem. Commun.* **1997**, 1705−1706.

(118) Nazeeruddin, M. K.; Pechy, P.; Renouard, T.; Zakeeruddin, S. M.; Humphry-Baker, R.; Comte, P.; Liska, P.; Cevey, L.; Costa, E.; Shklover, V.; Spiccia, L.; Deacon, G. B.; Bignozzi, C. A.; Grätzel, M. *J. Am. Chem. Soc.* **2001**, *123*, 1613−1624.

(119) Coulson, D. R. *Inorg. Synth.* **1971**, *13*, 121−124.

(120) One reviewer rightly noticed that the phthalocyanine triplet state is the lowest energy state in the dyads **5** and **6** and therefore could be the final excited state upon light excitation. Knowing that electron injection from the photoexcited ruthenium complex is a very fast process (in the range of 50 ps and even faster; see, for example, Benkö et al. *J. Am. Chem. Soc.* **2002**, *124*, 489), it could compete efficiently with the process that leads to a phthalocyanine triplet state.

4,4-Difluoro-8-5-[4′-phenyl-(2,2′:6′,2″-terpydin-4′-yl)]-1,3,5,7-tetramethyl-4-bora-3a,4a-diaza-*s*-indacene (13). Route A: A round-bottomed flask was charged with stannyl terpyridine **7** (200 mg, 050 mmol), bodipy-I **8** (250 mg, 0.6 mmol), $Pd_2dba_3-CHCl_3$ (52 mg, 50 μmol), tri-*tert*-butylphosphine (0.3 mL, 1.1 mmol), cesium fluoride (169 mg, 1.1 mmol), and 30 mL of dioxane. The mixture was degassed under argon and refluxed for 15 h. The solvents were rotary evaporated, and the residue was purified by column chromatography on alumina eluted with the mixture petrol ether/dichloromethane/triethylamine = 180/60/10, affording 100 mg (36%) of **7** as a bright orange solid.

Route B: A round-bottomed flask was charged with bromoterpyridine **10** (130 mg, 0.4 mmol), bodipySnMe$_3$ **11** (41 mg, 0.04 mmol), $Pd_2dba_3-CHCl_3$ (134 mg, 0.88 mmol), tri-*tert*-butylphosphine (0.22 mL, 0.88 mmol), cesium fluoride (134 mg, 0.88 mmol), and 30 mL of dioxane. The mixture was degassed under argon and refluxed for 15 h. The solvents were rotary evaporated, and the residue was purified by column chromatography on alumina eluted with the mixture petrol ether/dichloromethane/triethylamine = 180/60/10, affording 130 mg (58%) of **7** as a bright orange solid.

^{1}H NMR ($CDCl_3$, 300 MHz): δ 8.79 (s, 2H), 8.75 (dd, J = 1.8 and 4.8 Hz, 2H), 8,71 (d, J = 7.8 Hz, 2H), 8.03 (d, J = 8.4 Hz), 7.91 (ddd, J = 1.8, 7.5, and 7.8 Hz, 2H), 7.46 (d, J = 8.4 Hz, 2H), 7.39 (ddd, J = 1.2, 4.8, and 7.5 Hz, 2H), 6.01 (s, 2H), 2.57 (s, 6H), 1.41 (s, 6H). MS (EI): m/z (%) 555.30 (100, $M^{\bullet+}$), 535.35 (17). Anal. Calcd for $C_{20}H_{28}Cl_2N_2O_6S_2Ru$: H, 5.08; C, 73.52; N 12.61. Found: H, 5.11; C, 73.62; N, 12.51.

2,2′:6′,2″-Terpyridin-4′-yl Tri-*tert*-butylphthalocyaninatozinc-(II) (14). A sealed tube was charged with **12** (50 mg, 0.055 mmol), 4′-bromoterpyridine **10** (20 mg, 0.06 mmol), tetrakis(triphenylphosphine)palladium(0) (6 mg, 4 μmol), and 5 mL of dioxane. The mixture was degassed under argon and was refluxed for 15 h. The solvents were evaporated, and the crude was purified by preparative TLC (silica gel) eluted with the mixture dichloromethane/methanol = 9/1. The third blue band was isolated and washed with the mixture dichloromethane/dioxane/methanol = 7/2/1, affording 10 mg (18%) of the desired zinc phthalocyanine **14** as a blue solid.

^{1}H NMR ($CDCl_3$, 300 MHz): δ 8.72 (s, 2H), 8,70 (d, J = 5.0 Hz, 2H), 8.65 (d, J = 7.5 Hz, 3H), 8.59 (d, J = 8.0 Hz, 2H), 8.27 (s, 1H), 7.83 (m, 6H), 7.42 (m, 3H), 7.30 (m, 3H), 1.77 (s, 27H). HRMS (ES-MS): calcd for $C_{59}H_{49}N_{11}Zn$ ($M^{\bullet+}$), 975.3464; found, 975.3476.

Dichlorobis(dimethyl sulfoxide) [4,4′-(Diethoxycarbonyl)-2,2′-bipyridine]ruthenium(II) (18). $Ru(DMSO)_4Cl_2$ (500 mg, 1.03 mmol) was dissolved in 10 mL of chloroform, and the mixture was refluxed. A solution of 4,4′-(diethoxycarbonyl)-2,2′-bipyridine (**17**; 310 mg, 1.0 mmol) dissolved in 5 mL of chloroform was added dropwise via a syringe to the above solution. The mixture was refluxed for an additional 15 h. The chloroform was rotary evaporated. The residue was purified by column chromatography on silica gel eluted with the mixture dichloromethane/methanol = 98/2. The faster-moving band (purple) corresponds to the trans isomer, and the next major band (orange) corresponds to the cis isomer. Both isomers were gathered, affording a brown powder (455 mg, 70%).

cis isomer. ^{1}H NMR ($CDCl_3$, 300 MHz): δ 10.06 (d, J = 5.7 Hz, 1H), 9.86 (d, J = 5.7 Hz, 1H), 8.80 (s, 1H,), 8.73 (s, 1H), 8.12 (dd, J = 1.5 and 5.7 Hz, 1H), 7.99 (dd, J = 1.5 and 5.7 Hz, 1H), 4.54 (q, J = 7.2 Hz, 4H), 3.53 (s, 6H), 3.23 (s, 3H), 2.74 (s, 3H), 1.39 (t, J = 7.2 Hz, 6H).

trans isomer. ^{1}H NMR ($CDCl_3$, 300 MHz): δ 9.92 (d, J = 5.7 Hz, 2H), 8.66 (s, 2H), 8.05 (dd, J = 1.5 and 5.7 Hz, 2H), 4.54 (q, J = 7.2 Hz, 4H), 3.06 (s, 12H), 1.39 (t, J = 7.2 Hz, 6H). HRMS (ES-MS): calcd for $C_{20}H_{28}O_6N_2Cl_2Ru$ ($M^{\bullet+}$ + Na^+), 650.97070; found, 650.97060. Anal. Calcd for $C_{20}H_{28}Cl_2N_2O_6S_2Ru$: H, 4.49; C, 38.22; N, 4.46. Found: H, 4.61; C, 37.82; N, 4.06.

General Procedure for the Complexation of Terpyridyl Ligands 10, 13, and 19 with the Ruthenium Complex 18. A flask was charged with **18** (290 mg, 0.46 mmol, 1.5 equiv), 10 mL of ethanol, and lithium chloride (65 mg, 1.55 mmol) initially dissolved in 0.2 mL of water. The mixture was degassed with argon and then heated to 100 °C. The terpyridinyl ligands **10**, **13**, and **19** (0.31 mmol, 1 equiv) were initially dissolved in ethanol (2 mL), and the resulting solution was added to the above refluxing solution. The mixture was refluxed for 15 h, and the solvents were rotary evaporated to dryness. The residue was purified by column chromatography on an alumina stationary phase. The red solid was dissolved in methanol, and a solution of aqueous KPF_6 was added. The precipitate was filtered, washed with water, and dried over a vacuum line.

a. Complex 1. Eluent for the chromatography: dichloromethane/methanol = 98.5/1.5. Yield: 73%. ^{1}H NMR ($CDCl_3$, 300 MHz): δ 10.64 (d, J = 5.7 Hz, 1H), 9.01 (s, 1H), 8.87 (s, 2H), 8.78 (d, J = 6.0 Hz, 1H), 8.73 (s, 1H), 8.37 (d, J = 5.7 Hz, 2H), 8.13 (d, J = 7.8 Hz, 2H), 7.88 (d, J = 5.7 Hz, 1H), 7.85 (d, J = 7.8 Hz, 2H), 7.65 (m, 2H), 7.52 (d, J = 5.7 Hz, 1H), 7.37 (d, J = 6.9 Hz), 7.20 (dd, J = 6.9 and 8.0 Hz, 2H), 4.64 (q, J = 7.2 Hz, 2H), 4.36 (q, J = 7.2 Hz, 2H), 2.17 (s, 3H), 1.58 (t, J = 7.2 Hz, 3H), 1.32 (t, J = 7.2 Hz, 3H). HRMS (ES-MS): calcd for $C_{38}H_{33}O_4N_5ClRu$ ($M^{\bullet+}$), 754.0771; found, 754.0777. Anal. Calcd for $C_{38}H_{33}ClN_5O_4PF_6Ru\cdot 2H_2O$: H, 3.82; C, 49.44; N, 7.59. Found: H, 3.96; C, 49.03; N, 7.38.

b. Dyad 3. Eluent for the chromatography: dichloromethane/methanol = 95/5. Yield: 72%. ^{1}H NMR ($CDCl_3$, 300 MHz): δ 10.60 (d, J = 6.0 Hz, 1H), 9.05 (s, 1H), 8.84 (s, 2H), 8.75 (s, 1H), 8.65 (d, J = 7.0 Hz, 2H), 8.40 (d, J = 6.0 Hz, 1H), 8.30 (d, J = 7.5 Hz, 2H), 7.96 (d, J = 5.1 Hz, 1H), 7.89 (dd, J = 8.1 and 8.1 Hz, 2H), 7.67 (d, J = 6.0 Hz, 1H), 7.57 (d, J = 7.5 Hz, 2H), 7.47 (d, J = 5.4 Hz, 2H), 7.19 (dd, J = 5.4 and 7.2 Hz, 2H), 6.04 (s, 2H), 4.65 (q, J = 7.2 Hz, 2H), 4.37 (q, J = 7.2 Hz, 2H), 2.54 (s, 6H), 1.60 (s, 6H), 1.58 (t, J = 7.2 Hz, 3H), 1.40 (t, J = 7.2 Hz, 3H). MS (MALDI-TOF): calcd for $C_{50}H_{44}BF_2N_7O_4ClRu$ ($M^{\bullet+}$), 992.22; found, 992.2. Anal. Calcd for $C_{50}H_{44}BPF_8N_7O_4ClRu\cdot 3H_2O$: H, 4.23; C, 50.41; N, 8.23. Found: H, 4.20; C, 50.21; N, 8.12.

c. Complex 20. Eluent for the chromatography: dichloromethane/methanol = 98/2. Yield: 84%. ^{1}H NMR ($CDCl_3$, 300 MHz): δ 10.52 (d, J = 5.7 Hz, 1H), 9.00 (s, 1H), 8.81 (s, 2H), 8.74 (s, 1H), 8.52 (d, J = 8.0 Hz, 2H), 8.36 (d, J = 5.7 Hz), 8.13 (d, J = 5.7 Hz, 1H), 7.90 (dd, J = 8.0 and 8.0 Hz, 2H), 7.77 (d, J = 5.7 Hz, 1H), 7.45 (d, J = 6.0 Hz), 7.21 (dd, J = 6.0 and 8.0 Hz, 2H), 4.63 (q, J = 7.2 Hz, 2H), 4.35 (q, J = 7.2 Hz, 2H), 1.58 (t, J = 7.2 Hz, 3H), 1.32 (t, J = 7.2 Hz, 3H). HRMS (ES-MS): calcd for $C_{31}H_{26}N_5O_4ClBrRu$ ($M^{\bullet+}$), 747.9900; found, 747.9915.

General Procedure for the Substitution of the Chloro by the Thiocyanato Ligand for the Complexes 1, 3, 6, and 20. A solution of Ru(Terpy-R)[Bpy(CO_2Et)$_2$]Cl_2 (0.045 mmol, 1 equiv), potassium thiocyanate (1 mmol, 20 equiv), 10 mL of ethanol, and 0.2 mL of water was refluxed for 10 h in the dark. The solvents were rotary evaporated, and the crude was purified by column chromatography over an alumina stationary phase. Finally, the red solid was dissolved in methanol, and a solution of aqueous KPF_6 was added. The precipitate was filtered, washed with water, and dried over a vacuum line.

a. Complex 2. Eluent for the chromatography: dichloromethane/methanol = 99/1. Yield: 76%. ^{1}H NMR ($CDCl_3$, 300 MHz): δ

10.61 (d, $J = 5.7$ Hz, 1H), 9.03 (s, 1H), 8.75 (d, $J = 6.0$ Hz, 1H), 8.65 (s, 1H), 8.47 (d, $J = 5.7$ Hz, 2H), 8.36 (d, $J = 5.6$ Hz, 1H), 8.13 (d, $J = 7.8$ Hz, 2H), 7.95 (d, $J = 8.8$ Hz, 2H), 7.87 (dd, $J =$ 7.8 and 7.8 Hz, 2H), 7.75 (d, $J = 5.8$ Hz, 1H), 7.50 (d, $J = 6.9$ Hz, 2H), 7.44 (d, $J = 8.8$ Hz, 2H), 7.18 (dd, $J = 6.9$ and 8.0 Hz, 2H), 4.64 (q, $J = 7.2$ Hz, 2H), 4.36 (q, $J = 7.2$ Hz, 2H), 2.17 (s, 3H), 1.58 (t, $J = 7.2$ Hz, 3H), 1.32 (t, $J = 7.2$ Hz, 3H). HRMS (ES-MS): calcd for $C_{39}H_{33}O_4N_6SRu$ ($M^{\bullet+}$), 783.1328; found, 783.1333. Anal. Calcd for $C_{39}H_{33}N_6O_4PF_6SRu\cdot 4H_2O$: H, 4.13; C, 46.85; N, 8.40. Found: H, 4.21; C, 46.66; N, 8.31. IR (KBr): ν(NCS) 2096 cm^{-1}.

b. Dyad 4. Eluent for the chromatography: dichloromethane/methanol = 95/5. Yield: 70%. ^1H NMR ($CDCl_3$, 300 MHz): δ 10.62 (d, $J = 6.0$ Hz, 1H), 9.03 (s, 1H), 8.88 (s, 2H), 8.67 (s, 1H), 8.65 (d, $J = 7$ Hz, 2H), 8.39 (d, $J = 6.0$ Hz, 1H), 8.29 (d, $J = 7.5$ Hz, 2H), 7.96 (dd, $J = 6.0$ Hz, 1H), 7.89 (dd, $J = 5.4$ and 7.0 Hz, 2H), 7.67 (d, $J = 6.0$ Hz, 1H), 7.57 (d, $J = 7.5$ Hz, 2H), 7.47 (d, $J = 5.4$ Hz, 2H), 7.19 (dd, $J = 5.4$ and 7.2 Hz, 2H), 6.05 (s, 2H), 4.65 (q, $J = 7.2$ Hz, 2H), 4.37 (q, $J = 7.2$ Hz, 2H), 2.54 (s, 6H), 1.60 (s, 6H), 1.58 (t, $J = 7.2$ Hz, 3H), 1.40 (t, $J = 7.2$ Hz, 3H). MS (MALDI-TOF): calcd for $C_{51}H_{44}BF_2N_8O_4SRu$ ($M^{\bullet+}$), 1015.03; found, 1015.0. Anal. Calcd for $C_{51}H_{44}BPF_8N_8O_4SRu\cdot 3H_2O$: H, 4.15; C, 50.46; N, 9.23. Found: H, 4.10; C, 50.11; N, 9.26. IR (KBr): ν(NCS) 2096.1 cm^{-1}.

c. Complex 21. Eluent for the chromatography: dichloromethane/methanol = 99.5/0.5. Yield: 83%. ^1H NMR (DMSO-d_6, 300 MHz): δ 10.00 (d, $J = 5.7$ Hz, 1H), 8.98 (s, 1H), 8.88 (s, 2H), 8.67 (s, 1H), 8.50 (d, $J = 8.0$ Hz, 2H), 8.42 (d, $J = 5.7$ Hz), 8.03 (d, $J = 5.7$ Hz, 1H), 7.90 (dd, $J = 8.0$ and 8.0 Hz, 2H), 7.59 (d, $J =$ 5.7 Hz, 1H), 7.46 (d, $J = 6.0$ Hz), 7.24 (dd, $J = 6.0$ and 8.0 Hz, 2H), 4.63 (q, $J = 7.2$ Hz, 2H), 4.35 (q, $J = 7.2$ Hz, 2H), 1.58 (t, $J = 7.2$ Hz, 3H), 1.32 (t, $J = 7.2$ Hz, 3H). HRMS (ES-MS): calcd for $C_{32}H_{26}N_6O_4BrSRu$ ($M^{\bullet+}$), 770.9963; found, 770.9956. IR (KBr): ν(NCS) 2097 cm^{-1}.

General Procedure for the Stille Cross-Coupling Reaction with the Metallosynthon 20 or 21. A sealed tube was charged with Ru(Terpy-Br)[Bpy(CO_2Et)$_2$]$(X)^+$ **20** (X = Cl) or **21** (X = NCS) (0.067 mmol), trimethyltin antenna **13** or **14** (0.08 mmol), dichloro(diphenylphosphoferrocene)palladium(II) (10 mg, 0.01 mmol), copper iodide (2.5 mg, 0.01 mmol), 0.5 mL of triethylamine, and 3 mL of DMF. The mixture was degassed with argon and heated to 60 °C for 6 h. The crude reaction was evaporated to dryness, and the residue was purified as indicated below.

a. Dyad 3. Purification by column chromatography over alumina eluted with the mixture dichloromethane/methanol = 95/5. Yield: 42%. For characterizations, see above.

b. Dyad 4. Purification by column chromatography over alumina eluted with the mixture dichloromethane/methanol = 95/5. Yield: 48%. For characterizations, see above.

c. Dyad 5. Purification by preparative TLC (silica gel) eluted with the mixture saturated KPF_6 acetone solution/dichloromethane = 70/30. The major dark blue band was isolated and recrystallized with dioxane/methanol, affording pure dyad **5** (54 mg, 52%).

^1H NMR (DMSO-d_6, 400 MHz): δ 10.62 (d, 1H); 9.93 (s, 2H), 9.72 (s, 1H), 9.65−9.30 (m, 8H), 9.26 (s, 2H), 8.70 (s, 1H), 8.56 (s, 3H), 8.36 (s, 3H), 8.17 (s, 2H), 7.95 (s, 2H), 7.76 (s, 1H), 7.65 (s, 2H), 4.65 (q, $J = 7.2$ Hz, 2H), 4.37 (q, $J = 7.2$ Hz, 2H), 1.77 (s, 27H), 1.58 (t, 3H), 1.40 (t, 3H). HRMS (ES-MS): calcd for $C_{75}H_{65}N_{13}ClO_4ZnRu$ ($M^{\bullet+}$), 1412.3306; found, 1412.3315. Anal. Calcd for $C_{75}H_{65}N_{13}ClO_4ZnPF_6Ru\cdot 2H_2O$: H, 4.36; C, 56.47; N, 11.41. Found: H, 4.47; C, 56.17; N, 11.11.

d. Dyad 6. Purification by preparative TLC (silica gel) eluted with the mixture saturated KPF_6 acetone solution/dichloromethane = 70/30. The major dark blue band was isolated and recrystallized with the mixture dioxane/methanol, affording pure dyad **6** (63 mg, 60%).

^1H NMR (DMSO-d_6, 400 MHz): δ 10.29 (s, 1H), 9.80 (m, 3H), 9.58 (s, 1H), 9.50−9.20 (m, 7H), 9.12 (m, 2H), 8.59 (s, 1H), 8.38 (m, 3H), 8.23 (dd, $J = 8.0$ and 8.0 Hz, 2H), 7.90 (d, 2H), 7.81 (d, 1H), 7.68 (m, 2H), 7.57−7.39 (m, 3H), 4.65 (q, $J =$ 7.2 Hz, 2H), 4.37 (q, $J = 7.2$ Hz, 2H), 1.77 (s, 27H), 1.58 (t, $J = 7.2$ Hz, 3H), 1.40 (t, $J = 7.2$ Hz, 3H). HRMS (ES-MS): calcd for $C_{76}H_{65}N_{14}O_4SZnRu$ ($M^{\bullet+}$), 1435.3369; found, 1435.3461. Anal. Calcd for $C_{76}H_{65}N_{14}O_4SPF_6ZnRu\cdot H_2O$: H, 4.22; C, 57.05; N, 12.26. Found: H, 4.36; C, 56.95; N, 12.06. IR (KBr): ν(NCS) 2094.7 cm^{-1}.

Acknowledgment. The authors are thankful to the Ivory-Coast Ministry of Research and Education for the fellowship of H.Z. Dr. Mohammed Boujtita is also gratefully acknowledged for his kind assistance with the electrochemical study. The authors also acknowledge financial support from the French Ministry of Research for the ACI "jeunes chercheurs" 4057 for the development of this project.

Supporting Information Available: Overlay of the electronic absorption spectra of **8**, **13**, and **19** and **9**, **14**, and **19** recorded in dichloromethane. Overlay of the electronic absorption of the ruthenium complexes **1** and **2** recorded in DMF. Overlay of the room-temperature emission spectra of **2** and **6** in DMF. Aromatic region of the ^1H NMR spectrum and attribution of the signals for compounds **1**−**6**, **13**, and **14**. $^1H-^1H$ correlation (COSY) for complexes **1** and **2**. MALDI-TOF of dyads **3** and **4**. ES-MS spectra of dyads **3**−**6**. This material is available free of charge via the Internet at http://pubs.acs.org.

IC050078M